N O T I C E

THIS DOCUMENT HAS BEEN REPRODUCED FROM MICROFICHE. ALTHOUGH IT IS RECOGNIZED THAT CERTAIN PORTIONS ARE ILLEGIBLE, IT IS BEING RELEASED IN THE INTEREST OF MAKING AVAILABLE AS MUCH INFORMATION AS POSSIBLE

NASA

Technical Memorandum 80594

An Empirical Polytrope Law for Solar Wind Thermal Electrons Between 0.45 and 4.76 AU: Voyager 2 and Mariner 10

E.C. Sittler, Jr. and J. D. Scudder

NOVEMBER 1979

National Aeronautics and
Space Administration

Goddard Space Flight Center
Greenbelt, Maryland 20771

AN EMPIRICAL POLYTROPE LAW FOR SOLAR WIND THERMAL ELECTRONS BETWEEN 0.45 AND 4.76 AU: VOYAGER 2 AND MARINER 10

by

E. C. Sittler, Jr.*
and
J. D. Scudder
NASA/Goddard Space Flight Center
Laboratory for Extraterrestrial Physics
Greenbelt, MD 20771

TO BE SUBMITTED TO: Journal of Geophysical Research

* NAS/NRC Postdoctoral Research Associate

ABSTRACT

Empirical evidence is presented that solar wind thermal electrons obey a polytrope law with polytrope index $\gamma = 1.175 \pm 0.03$ (3σ). The Voyager 2 and Mariner 10 data used span the radial range from 0.45 AU to 4.76 AU and have a large dynamic range in density (4 decades), and over one decade in temperature, which is crucial for an unambiguous determination of γ. We find that there is a large $\sigma \pm 50\%$ variation in the entropy like stream tube constant Σ relative to its best fit value Σ_o. For the Voyager 2 data set, which has 5831 hourly averages, this variation comprises a nearly unbiased statistical sample of log Σ relative to log Σ_o, thereby reducing systematic errors. A positive correlation on average between Σ and bulk speed is found, which does introduce systematic errors (σ 5%) in the determination of γ resulting in larger uncertainties than implied by a simple regression of log T_e vs log n. Our result supports the theoretical predictions by Scudder and Olbert (1979b) that solar wind thermal electrons in the asymptotic solar wind, should obey a polytrope law with polytrope index $\gamma = 1.16 \pm 0.06$ (3σ). It does not support the results reported by Feldman et al. (1978) for high speed streams where they find $\gamma = 1.45 \pm 0.15$ (3σ). We attribute this difference to the biased sample of stream tube constants Σ encountered in that limited study and/or the smaller dynamic range of density and temperature available to the 1 AU observer. Our results support: 1) the widespread impressions in the literature that solar wind electrons behave more like an isothermal than adiabatic gas; 2) the arguments put forward by Scudder and Olbert (1979a,b) that Coulomb collisions are the dominant stochastic process shaping observed electron distribution functions in the solar wind, and 3) the assignment of the interplanetary potential as equal to approximately seven times the temperature of the thermal electrons.

I. INTRODUCTION

Attempts to model the two-fluid solar wind expansions have either used the full electron and ion energy equation with Spitzer's formulation of thermal conduction (Hartle and Sturrock (1966)) or have simplified the energy equations by assuming two different polytropic laws for ions and electrons (Goldstein and Jokipii (1977) and V. J. Pizzo, private communication). Both of these approaches have fundamental difficulties. Concurrent with the existence of a Spitzer thermal conductivity is the necessary condition that the Coulomb free path over the scale length be much less than unity and that the system be slightly removed from (homogeneous) thermodynamic equilibrium with local Maxwellian velocity distribution functions; however, the observed distribution functions do not have this property. The second approach represents a considerable mathematical simplification of the fluid equations; however, they must be regarded as phenomenological. In addition, since any heat law can be imitated by a spatially varying polytropic index, γ, the use of a single constant γ represents an additional assumption of the specific form of the heat law, namely that the heat transport is implemented as an enthalpy flux (cf. Parker, 1963).

In this paper we present empirical evidence that between 0.4 and 5 AU the thermal portion (but not all) of the solar wind electron population obeys a polytrope relation. We also show that this functional relationship is a member of a broader class of possible laws required of a steady state, fully ionized plasma whose proper frame electric field is dominated by the polarization electric field. The empirically determined, thermodynamically interesting value of $\gamma \simeq 1.175$ is virtually that predicted ($\gamma = 1.1\bar{6}$) by the theoretical considerations of Scudder and Olbert (1979b). We thus provide strong, direct, empirical evidence for the nearly isothermal behavior of solar wind electrons as has been indirectly argued in the literature for some time (Burlaga et al. (1971), Hundhausen and Montgomery (1971), Hundhausen (1973)).

This polytrope relation for the thermal electrons refers to the bulk ($\gtrsim$ 95%) of the number density and $\gtrsim$ 75% of the total electron pressure. By contrast the heat flow vector requires an accurate description of all the electrons including that peculiar minority of particles which make the

electron velocity distributions function skewed in the proper frame. This group of particles is usually in the trans to extrathermal regime $\mathcal{E} > kT$: (observationally Montgomery et al. (1968), Scudder (1970), Montgomery (1972); theoretically Scudder and Olbert, (1979a), hereafer referred to as SO-I). For the structureless solar wind in the regime where conduction is not energetically important the electron thermodynamics may in first approximation be described by this polytrope relation. However, the detailed description of the initial coronal acceleration or dynamical interactions in structured flow at any distance requires a further elaboration of the actual heat law. In particular the inference that advection is the principle mode of internal energy transport for electrons in stream interaction regimes beyond 20-30 R_o is probably inappropriate. This may be seen since use of the polytrope law stream line by stream line, neglects the possibility that heat can be locally deposited along the stream tube in the form of heat without the correlative amount of density enhancement.

2. THEORETICAL BACKGROUND

Because electrons have a small inertia relative to ions, the proper frame electric field present in the steady state inhomogeneous solar wind expansion is inextricably connected to the thermodynamic forces upon these particles. The generalized Ohm's law is the governing relation between this electric field, $\vec{E}^*$, in the proper frame and the gradient of macroscopic variables which are the local thermodynamic forces. The relation is determined by the difference of the electron and ion momentum equations and in general is given by equation 1

$$\vec{E}^* \equiv \vec{E} + \frac{\vec{u} \times \vec{B}}{c} = -\frac{1}{n_e e} \operatorname{div} \underline{\underline{P}}_e + \frac{1}{n_e e} \vec{j}^* \times \vec{B} - \frac{m_e}{n_e e^2} \left.\frac{\delta \vec{j}^*}{\delta t}\right|_{coll}$$
$$- \frac{m_e}{n_e e^2} \left[\frac{d}{dt} \vec{j}^* + \vec{u} \nabla \cdot \vec{j}^* + \vec{j}^* \cdot \nabla \vec{u} + \eta \left(\frac{d\vec{u}}{dt} - \vec{g} \right) \right] \qquad (1)$$

where, $\vec{E}$ and $\vec{E}^*$ are the electric field in the inertial and proper frame, respectively, $\vec{B}$ the magnetic field, $\vec{u}$ the proper frame velocity, $\underline{\underline{P}}_e$ the electron pressure tensor, n_e the electron density, $\vec{j}^*$ the proper frame current density, η the free charge density, $\vec{g}$ the gravitational force per unit mass, e the unit electric charge, m_e the

electron mass, and $\frac{d}{dt} = \frac{\partial}{\partial t} + \vec{u} \cdot \nabla$ is the total time derivative.

The terms on the RHS of Eq. 1 have been written in decreasing order of usual importance in the steady state solar wind as argued in Rossi and Olbert (1970), where most notably the first three terms are, respectively, the polarization, Hall, and collisional (or Ohmic heating) terms. The remaining set of terms are usually negligible in astrophysical circumstances.

The collisional group may be dropped since it is inversely proportional to the magnetic Reynolds number which is large in the solar wind. The size of the Hall term has been estimated assuming Alfvénic fluctuations and shown to be small ($\lesssim$ 10%) relative to the polarization term except, possibly in the lower corona.

In this section we will explore the implications of $\vec{E}^*$ being predominately determined by the polarization term.

$$\vec{E}^* = -\nabla \cdot \underline{\underline{P}}_e / en_e \qquad (2)$$

Using an argument made by S. Olbert (private communication, 1978) the curl free nature of $\vec{E}^*$ in steady state with $\underline{\underline{P}} \simeq P_e \underline{\underline{I}}$ and Eq. 2 implies that

$$\nabla \times \vec{E}^* = 0 \simeq \nabla \times \frac{(-\nabla \cdot \underline{\underline{P}}_e)}{en_e} \lesssim \nabla \times \frac{(-\nabla P_e)}{en_e} = + \frac{1}{en_e^2} (\nabla P_e) \times (\nabla n_e) \qquad (3)$$

Therefore, $P_e = f(n_e)$ is the most general relation which satisfies this requirement. A <u>particular</u> example of such a function $f(n_e)$ is the polytrope law

$$P_e = \Sigma \, n_e^{\gamma} \qquad (4)$$

where Σ is a stream tube constant and γ the polytrope index. However, without further justification there appears no rationale other than simplicity that a polytrope relation such as (4) should be <u>the</u> particular function f observed to relate thermal electron temperature and ambient density which satisfies (3).

The properties of the velocity dependence of Coulomb scattering were examined in Scudder and Olbert (1979b), hereafter referred to as SO-II

where it was shown both theoretically and empirically that a change in the solar wind electron velocity distribution function occurs in the vicinity of a transition energy $\mathcal{E}^* = 7\ kT_c$, where T_c is the "temperature" of the thermal (core) electrons; the constant 7 only depended on fundamental constants (m_e, m_p, e, and that $T_e \lesssim T_p$). These authors explored the implications that this dimensionless transition energy $\mathcal{E}^*/kT_c$ could be independent of space and time while $\mathcal{E}^*$ was simultaneously the interplanetary potential suggested by exosphere approaches to the solar wind electron theory: (Jockers (1970); Schultz and Eviatar (1972); Perkins (1973)) and observations: (Feldman et al. (1975), Rosenbauer et al. (1976)). It was concluded in SOII that the necessary and sufficient condition that this be possible is that the thermal electrons do obey a polytrope law, Eq. 4, with an expected $\gamma = 1.16 \pm 0.06$ (3σ). We now proceed to test their conclusions.

3. SOLAR WIND ELECTRON OBSERVATIONS VOYAGER 2 - MARINER 10

The simplest manner of empirically determining γ would be a linear least squares fit of the two observables log T_c versus log n_e with best slope, α_{fit}, and its uncertainties being identified with γ by

$$\gamma = \alpha_{fit} + 1 \tag{5}$$

Because the variation of T_c with radius previously reported by Gringauz and Verigin (1975) Ogilvie and Scudder (1978) and Sittler et al. (1979) is so shallow, obtaining a significant dynamic range in temperature (greater than one order of magnitude) requires a protracted period of data collection for a deep space mission such as Voyager. The Voyager results to be discussed have been derived from data collected by a cylindrical Faraday cup between 1.38 and 4.76 AU over a period of 1 1/3 years, or about 18 solar rotations. These data span one order of magnitude variation in thermal temperature and three orders of magnitude in density. The Mariner 10 data were collected by a spherical section electrostatic analyzer between 0.9 and 0.45 AU over a period of 2 months. These data extend the composite data coverage to nearly four orders of magnitude in density and over an order of magnitude in thermal electron temperature. (Further details of Voyager and Mariner 10 processing and experimental assumptions are described in

(Sittler and Scudder (1979) and Ogilvie and Scudder (1978); the Voyager instrument is described in detail in Bridge et al., 1977)).

Because neither of the variables in the suggested relation (4) are determined with absolute precision, the linear least squares approach for determining γ is inadequate. The more general approach of "hypothesis testing" (Eadie et al., (1971)) is required whereby the perpendicular dispersion of the data from the optimal hypothesis is minimized. This procedure corresponds in this case to determining the polytrope constant Σ (intercept) and index γ = (slope + 1) in a way that minimizes the perpendicular dispersion of our observations relative to this hypothesized law. In log-log space the polytrope hypothesis along each stream tube labeled "s" is a straight line

$$\log T(s) = \alpha_{fit} \log n(s) + \log \Sigma(s) \qquad (6a)$$

$$\equiv \alpha_{fit} \log n(s) + I(s) \qquad (6b)$$

with slope α_{fit} and intercept I. Minimizing the perpendicular dispersion about this hypothesis is particularly simple.

Voyager 2 Data

We have performed this minimizing procedure on the Voyager data and the results are shown in Figure 1. In the body of the figure is plotted the optimal polytrope hypothesis with empirical polytrope index $\gamma = \alpha_{fit} + 1 = 1.185 \pm 0.018$ (3σ) and with optimal average stream tube constant $\langle \log \Sigma \rangle = I$ given by 4.74 ± 0.009 (3σ) where the units of Σ are determined by T (°K) and n (cm^{-3}). Each cross represents the mean determined from the Voyager 2 hourly averaged data points which are found in bins perpendicular to and of equal width along the best fit line. The 5831 Voyager hourly data points were used to determine the optimal polytrope relation. As a group the binned data points and error bars (in many cases error bars are smaller than the size of the crosses) closely resemble the polytrope relation selected by the above described minimization process. The error flags are parallel to the sides of the bins which the optimal hypothesis slope defines, being perpendicular to the selected best hypothesis line. (These lines do not appear perpendicular

since decades of density and temperature do not have the same physical dimension in the figure). It is, however, clear that attempts to determine the best fit line for subsets of the data with smaller than the current dynamic range could determine slopes that are grossly inconsistent with the trend of the composite set (cf. Feldman et al., 1978).

Mariner 10 Data

The solid dots in Figure 1 show the placement of all similarly binned hourly averaged Mariner 10 electron data in this log T, log n space. The Mariner 10 data taken in 1973 had a slightly higher average stream tube constant $I_{M10} = 4.83$ than for the average Voyager data ($I_{Voyager} = 4.74 \pm 009\ 3\sigma$). The Mariner 10 data have been placed on this figure so that as a set they have the same average stream tube constant as obtained by the Voyager fit. This has been done by a slight ($\lesssim 1\%$) displacements of the direct observations perpendicular to the average Voyager polytrope fit relation. The Mariner 10 data points clearly follow the trend suggested by the Voyager data set and give further dynamic range to the empirical relation.

In inset 1A of Figure 1 we address the uncertainty with which the polytrope constant $< \log \Sigma >$ and index $\gamma = \alpha_{fit} + 1$ have been determined. The panel is comprised of a gray scale map of the χ^2 surface in the vicinity of the optimal $< \log \Sigma >$ and α_{fit} selected by the non-linear least squares procedure outlined above. Motion parallel to the horizontal axis corresponds to changing the slope of the hypothesis while keeping the intercept fixed. Motion along the ordinate corresponds to changing the intercept while keeping the slope fixed. The gray coded intensity corresponds to the magnitude of χ^2, the normalized mean square dispersion of the data about a polytrope hypothesis, with polytrope constant and index determined by its location on the χ^2 map. The variation of χ^2 in increments of intensity from 0 to 15 is given by

$$\chi^2 = \begin{cases} 15 \dfrac{\chi^2 - \chi^2_{min}}{\chi^2_{max} - \chi^2_{min}} + 1 \text{ for } \chi^2_{min} < \chi^2 \leq \chi^2_{max} \\ 0 \text{ for } \chi^2 = \chi^2_{min} \end{cases}$$

where $\chi^2_{min} = 7.07$ and $\chi^2_{max} = 8.08$. Using the procedure discussed by Lampton et al. (1976), the 99% confidence level occurs just inside the $\pm 3\sigma$

range of the plot (where σ has been defined by the linear least squares fit to the binned data. It is particularly important to note that there are no topological "channels" in the χ^2 surface that lead away from the optimally selected α_{fit} and I which are found to be at the bottom of a nearly circular well in the dispersion surface. This is not a foregone conclusion because of the non-linear character of the minimization process.

It is appropriate to document the distribution of the Voyager observations in the T, n space as available from the spacecraft time series. This has been graphically done in inset B of Figure 1. The central square panel of inset 1B depicts the intensity keyed probability $P_j\ (D_{ij}/\sigma_j)$ of departure of individual hourly averaged observations from the optimal polytrope relation shown in the main figure. σ_j is the variance of all the displacements D_{ij} in the jth bin. The horizontal axis (or bin index j) is measured in units along the best fit line of the main figure. For every cross in the main figure there corresponds 3 vertical columns (bins) in the central and lower panel of inset 1B. All observations were found to be confined to $\pm 3\sigma$; of the optimal position. The intensity keyed probability distribution P_j in each column (bin) represents the observed normalized frequency of departure within each bin of the stream tube constant $\Sigma(t)$ sampled by Voyager relative to the average $< \Sigma(t) >$ determined from the composite fit.

The upper horizontal panel gives the 16 linearly graded levels of intensity for the probability of occurrence. The lower horizontal panel gives the percent of the total Voyager data set within each bin, where the blank keys represent less than 29 observations within each bin while typically there are $\sim$ 170 observations within each bin.

The vertical steps to the right of the central panel depicts in normal histogram form the composite distribution of stream tubes constants sampled. This composite is defined as

$$P\ (D\ /\sigma) = \frac{1}{N_T} \sum_{j=1}^{N_B} n_j\ P_j\ (D_{ij}/\sigma_j) \qquad (6)$$

where N_T is the total number of observations, n_j the total number of points in each bin, and N_B the number of bins.

Inset Figure 1B documents the following: (1) (in the central panel) that the most aberrant points from the polytrope law are from data obtained over short enough time to have a biased set of stream tube constants for the regime encountered (the first three points of main Figure 1 come from a sparse high velocity stream at 4.76 AU at the very end of our time series); these data are thus strongly coherent and not statistically representative of stream tube constants for this density regime; (2) (lower strip) these biased data points are not dominant in determining our optimal polytrope; (3) adjacent subsets of bins over a small dynamic range may or may not have gaussian $P_j\ (D_{ij}/\sigma_j)$, i.e., impartial samples of stream tube constants; and (4) (right strip) that the entire data set as a whole represents a nearly statistically unbiased sample of stream tube constant regimes (i.e., note gaussian shape of composite $P(D_i/\sigma)$ where $P(1) \sim 1/e$). To illustrate this result we have compiled in Figure 2 a plot of the percent of occurrence of $\log \Sigma$ as determined by hourly averaged $\log (T_i/(n_i^{-\alpha_{fit}}))$ with mean value $\langle \log \Sigma \rangle = 4.74$. The near gaussian shape with 1σ width $\sim 50\%$ of $\langle \Sigma \rangle$ shown here, means the data set is comprised of a nearly statistically random distribution of $\log \Sigma$. However, as the equal variance reference gaussian curve of the figure illustrates, the sample does have a slight shewness in the sample frequencies of $\log \Sigma$.

The fourth conclusion above and Figure 2 suggest that the composite Voyager data represent a nearly statistical sample of stream tube constants with respect to the "typical" best fit line which gives the average stream tube constant $\Sigma_o = 10^I$. Before the mathematically defined best fit slope, α_{fit}, is interpretable as the thermodynamically interesting, physical, polytrope index <u>along</u> a given stream tube, we must quantify the degree of correlation present in the data between stream tube constants sampled and the density.

4. <u>FITS AND PHYSICS</u>

We must now focus on the interpretation of the fits presented in relation to our assumed model. The fits pertain to data collected <u>across</u> many different stream tubes in the solar wind, whereas the hypothesis being tested pertains to the physics of thermal electrons <u>along</u> each stream tube. This distinction is basic since there exists no <u>a priori</u> theoretical

relationship which can suggest how such a "cross tube" sample should appear in the fits previously presented.

Our working hypothesis is to test the idea of SO-II that thermal electrons, along the arc length ℓ of the stream tube labeled by s, obey the hypothesis $\log T(s,\ell)) = \alpha \log n(s,\ell) + \log \Sigma(s)$, where α is a constant independent of stream tube, but $\Sigma(s)$ may change in some way across tubes as boundary conditions prescribe. From this relation it follows that

$$\frac{d}{dt} \log T(s(t),\ell(t)) = \alpha \frac{d}{dt} \log n(s(t),\ell(t)) + \frac{d}{dt} \log \Sigma(s(t)) \qquad (7)$$

where the time derivatives are those determined by the time series encountered by the detector as provided by the combined motion of the spacecraft and the bulk flow of the medium between 1.38 and 4.76 AU. The last expression of (7) vanishes only when the above motion carries the detector along the stream tubes in the flow, and certainly does not vanish in any average sense over the protracted time series considered here. Rearrangement of equation (7) and noting the properties of total derivatives we obtain

$$\frac{d \log T(s(t),\ell(t))}{d \log n(s(t),\ell(t))} = \alpha + \frac{d \log \Sigma(s(t))}{d \log n(s(t),\ell(t))}, \qquad (8)$$

where, as before, the last term is in general non-vanishing.

The fitting procedure described in the previous section "characterizes" the average value of the left-hand side of (8). Let us denote this procedure by the angular brackets $\langle\ \rangle$; we thus identify

$$\alpha_{fit} \equiv \left\langle \frac{d \log T(s(t),\ell(t))}{d \log n(s(t),\ell(t))} \right\rangle = \alpha + \left\langle \frac{d \log \Sigma(s(t))}{d \log n(s(t),\ell(t))} \right\rangle \equiv \alpha + \beta(\alpha). \qquad (9)$$

The non-vanishing size of the last term in (9), which we have defined as β, complicates the simple identification of α_{fit} with the physically interesting quantity α of our hypothesis. The magnitude of β must be assessed before the size of α or its precision may be determined.

The quantity β is not only a function of n and T but also α, the physical variable. We initially assume that $\alpha \overset{\sim}{>} \alpha_{fit}$ to gauge the size of $\beta(\alpha) \overset{\sim}{>} \beta(\alpha_{fit})$; however, if β makes a sizeable correction to α_{fit}, this may

not be an accurate approximation. As shown in Table 1 the value of $\langle\beta(\alpha_{fit})\rangle$ (as determined by minimizing perpendicular dispersion of linear hypothesis α_{fit} relating log Σ and log n) for all the data used in Figure 1 is 30% of α_{fit}. We thus conclude that α_{fit} of Figure 1 is not exactly the best value to determine the polytrope index.

Among the physical correlations involved in determining the average size of $\beta(\alpha)$ in our sample are at least the following:

$$\beta(\alpha) = \left\langle \frac{d \log \Sigma(\alpha, s(t))}{d \log n(s(t), \ell(t))} \right\rangle = \left\langle \frac{\partial \log \Sigma}{\partial \log u} \frac{\partial \log u}{\partial \log n} \right\rangle + \left\langle \frac{\partial \log \Sigma}{\partial \log \alpha} \frac{\partial \log \alpha}{\partial \log u} \frac{\partial \log u}{\partial \log n} \right\rangle + \ldots, \tag{10}$$

which says that β may be comprised of non-zero average dependences of Σ on flow velocity u, density n, or with polytrope index via its bulk speed dependence. Since u and n are strongly correlated (Neugebauer and Snyder (1966); Burlaga and Ogilvie (1970)), it is unlikely in any given data collection that $\partial \log u / \partial \log n$ averages to zero. The next two entries in Table 1 show the values of α_{fit}, I, and $\beta(\alpha_{fit})$ for two disjoint speed subsets of the composite data: $u \lesssim 400$ km/s. The α fit values of these subgroups differ from that of the composite group by $\lesssim 11\%$ whereas the β values have been reduced more than 200%. The χ^2_{min} shown in Table 1 have also been significantly reduced. However, the average stream tube constants $\Sigma = 10^I$ have also changed significantly and there is a clear distinction between $\Sigma(u > 400)$, and $\Sigma(u \leq 400)$ with Σ larger in the high speed flow. (The errors quoted in Table 1 are 3σ errors.) This is also consistent with $(\Sigma_{M10}) > (\Sigma_{Voyager})$ since the Mariner 10 epoch had a higher average speed than the Voyager interval (cf. SO-II and Sittler et al., 1979). The α fit values of the two speed subgroups are identical even at the 1σ confidence level. We therefore conclude that

$$\frac{\partial \log \Sigma}{\partial \log u} \quad \text{is} > 0 \tag{11}$$

that

$$\frac{\partial \log \alpha}{\partial \log u} \lesssim 0 \tag{12}$$

and that the complications implicit in (10) are somewhat alleviated by narrowing the speed dispersion of the sample.

The results of equation (11) and (12) and the density-bulk speed anti-correlation noted above imply that β_{fit} should be expected to be negative provided there are no unexplored functional dependences in equation (10) (+.....). The negative fit values of β are therefore compatible with the initial fits which determine α_{fit} and I for the two speed subgroups. It is worth emphasizing that equation (11) implies that the entropy-like quantity Σ is positively correlated with the local bulk velocity.

Fortunately the data set $u \leq 400$ km/s has a very small systematic residual, $\beta(\alpha_{fit})$, and in this case $\alpha \overset{\sim}{\sim} \alpha_{fit} - \beta(\alpha_{fit}) \sim 0.175$. We use this to refine our estimates of β for all data subgroups since β is a function of the physical α. This has been done in the ninth column of Table 2. The revised values of α determined in this manner are given in the eleventh column. This last entry has been omitted for the first row since the composite data set has the largest systematic β and the worst normalized χ^2 of all the entries in this table. The second and third rows of this table yield a weighted average α of $\bar{\alpha} = 0.185 \pm 0.015$ (1σ) $\pm$ 0.045 (3σ) where we have assigned the one sigma uncertainty to correspond to the ($\pm$) offsets of α required to attain the mean values of data subsets (2) or (3).

The fourth row in Table 1 illustrates that the above errors are reasonable by repeating our procedure for the most frequently observed bulk speed interval (350-400 km/sec) with an estimated physical $\alpha_{350-400} = 0.205 \pm 0.034$ (3σ), which is almost completely contained in the (3σ) confidence interval of $\bar{\alpha}$ given above.

We estimate that the most probable value is $\alpha = 0.175 \pm 0.030$ (3σ) based on small systematic correction required in data grouping (2) of Table 1; we have determined a (3σ) confidence interval to not exclude any χ^2 defensible estimate of α. In view of the systematic corrections required in groups (3) and (4) we do not believe the present data support any significant variation of α with bulk speed.

SUMMARY

In summary we have come to the following conclusions:

(1) The experimental results presented here unambiguously support the widespread impression in the literature (e.g., Burlaga et al. (1971);

Hundhausen and Montgomery (1971); Hundhausen (1973), that the high electron mobility in the solar wind allows electrons to behave more like an isothermal than adiabatic gas;

(2) Our results give further experimental support to the arguments in SO-II that 7 $kT_e(r)$ is nearly the local interplanetary potential $e\Phi(r)$, since a polytrope law with $\alpha = 1/6$ was a necessary and sufficient condition for this result. In Figure 3 we graphically exhibit the confidence windows for the various suggestions of α made to date. The 99.9% confidence intervals of the Voyager fit data of the current work does have a sizeable overlap with the corresponding 99.9% confidence intervals of α suggested by Scudder and Olbert (1979b).

(3) Indirectly our results also imply that the proper frame electric field beyond at least 0.45 AU is dominated by the polarization term.

(4) As also shown in Figure (3) the Voyager-Mariner 10 empirical results are incompatible at greater than the 99.9% level of confide with a 99.9% confidence interval of $\alpha = .45$ recently reported by Feldman _et al_. (1978). We attribute this difference to the possible biased sample of stream tube constants (d log Σ/d log n) encountered in that limited study and/or the smaller dynamic range of the variables available to the 1 AU bound observer. (In the IMP study, the dynamic range of the density was a factor of five (5) and only high speed flows were considered. Note that the higher speed Voyager subset of Table 1 is also completely incompatible with the IMP results).

(5) Our composite data set indicates that on a statistical basis the one e-folding of the stream tube constant Σ is found to occur at $\stackrel{\sim}{>}$ 50% of the typical value with larger stream tube constants being more typical of higher speed flows. This sense and magnitude of stream tube constant variation was that suggested in SO-II to reconcile $\gamma = 7/6$ of theory with $\gamma = 1.45$ reported by Feldman _et al_. (1978).

(6) The suggested value of $\gamma = 7/6$ made in SO-II is most sensitive to an accurate description of the lowest two _even_ moments, n_e, P_e, of the electron velocity distribution. These moments are dominated respectively at approximately the 95 and 75% levels by the contributions from the thermal regime electrons. It is inconsistent to infer from our results that the heat flow which is an odd moment over _all_ the electrons is an enthalpy flux. The heat flux is controlled microscopically by the

asymmetrical distribution in velocity space of the trans- and extrathermal electrons (SO-I) which comprise a small fraction of the density and pressure. Therefore, this empirical corroboration of the polytrope law for thermals sheds no direct light on the control of the peculiar, non-dominant fraction of the electron phase space which actually implements the heat flow of the medium. Rather, these data highlight the control the thermal electrons have on the polarization potential which in turn is an important force in the subsequent balance of forces which determines the heat flow.

ACKNOWLEDGMENTS

The data analyzed in this paper were obtained by plasma instruments developed for Mariner 10 and Voyager space probes as part of experimental collaborations between NASA/GSFC and MIT under the leadership of H. S. Bridge, Principal Investigator. To him we both owe a deep debt of appreciation for the opportunity to analyze these novel data sets; we are also indebted to the remaining Co-Investigators for allowing us to participate in this way in these mission opportunities. In particular we appreciate discussions with and/or manuscript comments from Drs. Stanislaw Olbert, Leonard Burlaga, Keith Ogilvie, and Y. C. Whang. The large volume of data processed here would not have been possible without the substantive parallel analysis of the Voyager ion data under the direction of Dr. J. W. Belcher, MIT, as well as the batch data efforts of M. Harrision, CSC/GSFC, L. Moriarity and S. Beckwith of the NASA/GSFC, Laboratory for Extraterrestrial Physics, Information Analysis & Display Office, under the supervision of W. H. Mish.

REFERENCES

Bridge, H. S., J. W. Belcher, R. J. Butler, A. J. Lazarus, A. M. Mavretic, J. D. Sullivan, G. L. Siscoe, and V. M. Vasyliunas, "The Voyager Plasma Science Experiment, Space Sci. Rev., 21, 259-287, 1977.

Burlaga, L. F. and K. W. Ogilvie, "Magnetic and Thermal Pressures in the Solar Wind", Solar Phys., 15, 61, 1970.

Burlaga, L. F., K. W. Ogilvie, D. H. Fairfield, M. D. Montgomery, and S. J. Bame, "Energy Transfer of Colliding Streams in the Solar Wind", Astrophys. J., 164, 137, 1971.

Eadie, W. T., D. Drijard, F. E. James, M. Roos, and B. Sadoulot, Statistical Methods in Experimental Physics, North Holland Publishers, Amsterdam, Holland, 1971.

Feldman, W. C., J. R. Asbridge, S. J. Bame, M. D. Montgomery, and S. P. Gary, "Solar Wind Electrons", J. Geophys. Res., 80, 31, 1975.

Feldman, W. C., J. R. Asbridge, S. J. Bame, J. T. Gosling, and D. S. Lemons, "Electron Heating within Interaction Zones of Simple Solar Wind High Speed Streams, J. Geophys. Res., 13, 5297, 1978.

Goldstein, B. E. and J. R. Jokipii, "Effects of Stream-Associated Fluctations upon the Radial Variation of Average Solar Wind Parameters", J. Geophys. Res., 82, 1095, 1977.

Gringauz, K. I. and M. I. Verigin, "Electron Temperature Radial Distribution in the Solar Wind and Solar Wind Models", Space Research Institute, Academy of Sciences, USSR, preprint D 218, 1975.

Hartle, R. E. and P. Sturrock, "Two-fluid Model of the Solar Wind", Astrophys. J., 151, 1155, 1968.

Hundhausen, A. J. annd M. D. Montgomery, "Heat Conduction and Non-Steady Phenomenon in the Solar Wind", J. Geophys. Res., 76, 2236, 1971.

Hundhausen, A. J., "Solar Wind Stream Interactions and Interplanetary Heat Conduction", J. Geophys. Res., 78, 7996, 1973.

Jockers, K., "Solar Wind Models Based on Exospheric Theories", Astron. Astrophys. 6, 219, 1970.

Lampton, M., B. Margon and S. Bowyer, "Parameter Estimation in X-Ray Astronomy", Astrophys. J., 208, 177, 1976.

Montgomery, M. D., S. J. Bame, and A. J. Hundhausen, "Solar Wind Electrons: Vela 4 Measurements", J. Geophys. Res., 73, 15, 4999, 1968.

Montgomery, M. D., "Thermal Energy Transport in the Solar Wind", in Cosmic Plasmas, K. Schindler, ed., Plenum Press, New York, 1972.

Neugebauer, M. and C W. Snyder, "Mariner 2 Observations of the Solar Wind, 1, Average Properties", J. Geophys. Res., 71, 4469, 1966.

Ogilvie, K. W. and J. D. Scudder, "The Radial Gradients and Collisional Properties of Solar Wind Electrons", J. Geophys. Res., 83, 3776, 1978.

Parker, E. N., Interplanetary Dynamical Processes, J. Wiley Interscience, New York, 1963.

Perkins, R. W., "Heat Conductivity, Plasma Instabilities and Radio Star Scintillations in the Solar Wind", Astrophys. J., 179, 637, 1973.

Rosenbauer, H., H. Miggenreider, M. Montgomery, and R. Schwenn, "Preliminary Results of the Helios Plasma Measurements", in Physics of Solar Planetary Environaments, Proc. ISSTP, 1, 319, D. J. Williams, ed., AGU Publ. 1976.

Rossi, B. and S. Olbert, Introduction to the Physics of Space, McGraw-Hill Book Co., New York 1970.

Schultz, M. and A. Evis , "Electron-Temperature Assymmetry and the Structure of the So . Wind", Cosmic Electrodynamics, 2, 402, 1972.

Scudder, J. D., in Solar Wind, NASA-SP-308, 211, 1970.

Scudder, J. D. and S. Olbert, "A Theory of Local and Global Processes which Affect Solar Wind Electrons, I: The Origin of Typical 1 AU Velocity Distribution Functions - Steady State Theory", J. Geophys. Res., 84, A6, 2755, 1979a.

Scudder, J. D. and S. Olbert, "A Theory of Local and Global Processes which Affect Solar Wind Electrons, II: Experimental Support", J. Geophys. Res., 84, A11, 1979b. (November JGR).

Sittler, E. C., Jr., J. D. Scudder, J. Jessen, "Radial Variation of Solar Wind Thermal Electrons between 1.36 and 2.25 AU: Voyager 2," in Solar Wind 4 Proceedings, Burghausen, Federal Republic of Germany. H. Rosenbauer, ed. To be published by Springer-Verlag 1979. Also available in NASA/GSFC TM 79711, February 1979.

Sittler, E. C., Jr. and J. D. Scudder, "Voyager Electron Results in the Interplanetary Medium between 1.36 and 5 AU", in preparation.

FIGURE CAPTIONS

FIGURE 1 Main figure depicts Voyager data (+) binned as described in the text and the optimal power law hypothesis they determine. The dots depict all Mariner 10 data as binned in relation to the Voyager relation. Error bars are mathematically perpendicular to the optimal hypothesis line since the averages and dispersions implied are those for the data found in bins along the best fit line.

(Inset 1A) depicts the χ^2 surface for the non-linear optimization which selected the coefficients of the line plotted in the main figure. This inset emphasizes that the local minimum selected is not topologically connected by a descending trough to other regimes in the parameter space even though the non-linear procedure does not guarantee that this need be true.

(Inset 1B) illustrates in the square box the actual probability distribution of individual hourly averaged Voyager points as a function of the normal distance (scaled by the variance within each bin, D/σ_B), from the best fit line selected in the main figure. The right hand vertical strip denotes the composite probability distribution of observations taken as a set regardless of bin location along the best fit line. The upper horizontal code exhibits the 16 level intensities used in the probability plots. The lower horizontal code illustrates the percentage distribution of the analyzed data in each bin. Three bins of inset 1B are used for each point in the main figure. Refer to the text for further details and interpretation.

FIGURE 2 The histogram illustrates the percent relative occurrence of stream tube constants Σ as a function of departures from the average value. The dashed curve depicts a gaussian

distribution of equal variance; the observed distribution has an e-folding value at ∿ 50% in excess of the typical value and is nearly, but not precisely, skew free. This feature of the data time series complicates statements of precision as discussed extensively in the text.

FIGURE 3 A comparison of confidence fit intervals as suggested by 1) the present *in situ* analysis between 0.45 and 4.76 AU, 2) the theoretical suggestion of Scudder and Olbert 1979b (SO-II), and 3) the recent *in situ* analysis at 1 AU by Feldman *et al*. (1978). With the aid of this figure a comparison can be made of the agreement or not that is manifest between alternate lines of reasoning. Above the 60% confidence level the present analysis and the regime suggested in SO-II are indistinguishable; at all but the highest levels of confidence the present results are incompatible with those suggested by Feldman *et al*. (1978).

TABLE 1

(all errors are 3σ)

	Class	# Data	χ^2	α_{fit}	$3\sigma_\alpha$	I	$3\sigma_I$	$\beta(\alpha_{fit})$	$3\sigma_{\beta(\alpha_f)}$	$\beta(0.170)$	$3\sigma_{\beta.170}$	α_{phys}	$3\sigma_{\alpha_{phys}}$
1)	All	5831	7.07	0.183	0.018	4.74	0.009	-0.070	0.010	-0.052	0.010	-	-
2)	$u \leq 400$	2801	1.67	0.165	0.015	4.72	0.020	-0.005	0.015	-0.010	0.015	0.175	0.021
3)	$u > 400$	3030	2.75	0.168	0.015	4.78	0.014	-0.035	0.015	-0.038	0.020	0.201	0.021
4)	$350 < u < 400$	1803	1.96	0.230	0.023	4.74	0.020	-0.035	0.025	+0.030	0.020	0.205	0.034

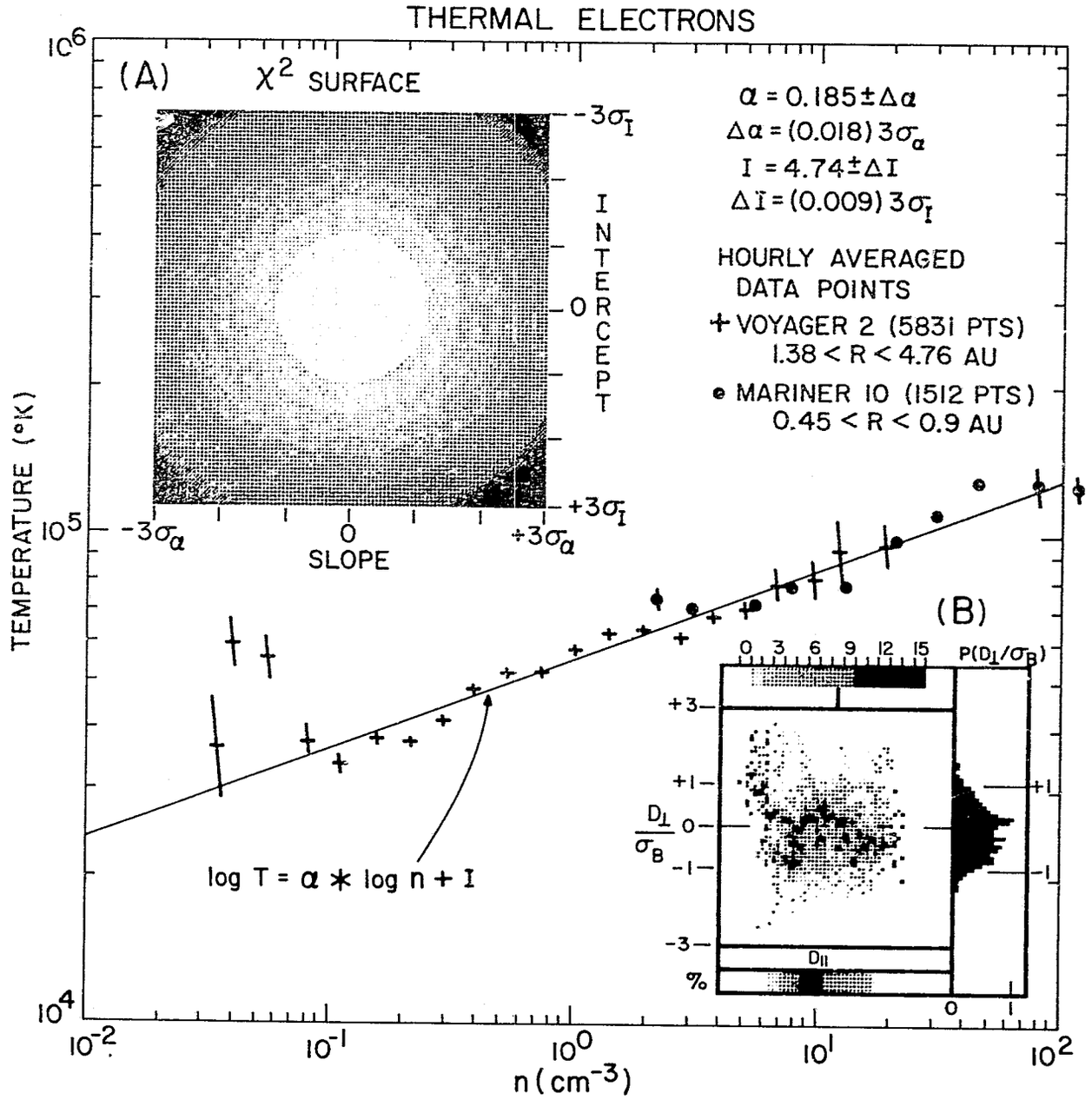
THERMAL ELECTRONS
(A) χ^2 SURFACE
$-3\sigma_I$
INTERCEPT
0
$+3\sigma_I$
$-3\sigma_\alpha$
0
SLOPE
$+3\sigma_\alpha$
$\alpha = 0.185 \pm \Delta\alpha$
$\Delta\alpha = (0.018)\,3\sigma_\alpha$
$I = 4.74 \pm \Delta I$
$\Delta I = (0.009)\,3\sigma_I$
HOURLY AVERAGED DATA POINTS
+ VOYAGER 2 (5831 PTS)
1.38 < R < 4.76 AU
• MARINER 10 (1512 PTS)
0.45 < R < 0.9 AU
TEMPERATURE (°K)
10^6
10^5
10^4
(B)
0 3 6 9 12 15 $P(D_\perp/\sigma_B)$
+3
+1
$\frac{D_\perp}{\sigma_B}$ 0
-1
-3
$D_\parallel$
%
0
1
+1
-1
log T = α * log n + I
10^{-2}
10^{-1}
10^0
10^1
10^2
n (cm^{-3})

Figure 1

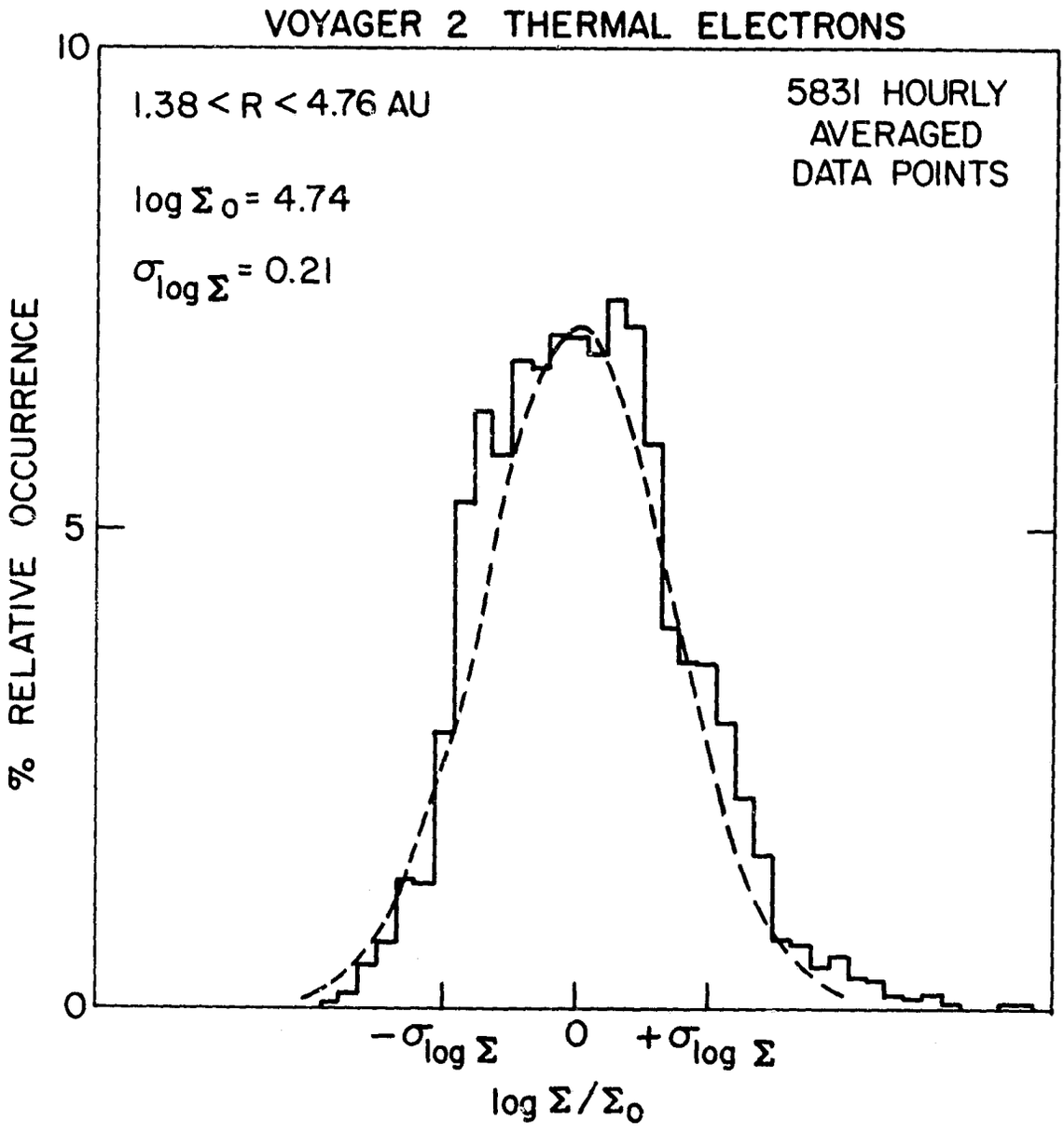
VOYAGER 2 THERMAL ELECTRONS
1.38 < R < 4.76 AU
5831 HOURLY AVERAGED DATA POINTS
log Σ0 = 4.74
σlog Σ = 0.21
% RELATIVE OCCURRENCE
10
5
0
−σlog Σ
0
+σlog Σ
log Σ/Σ0

Figure 2

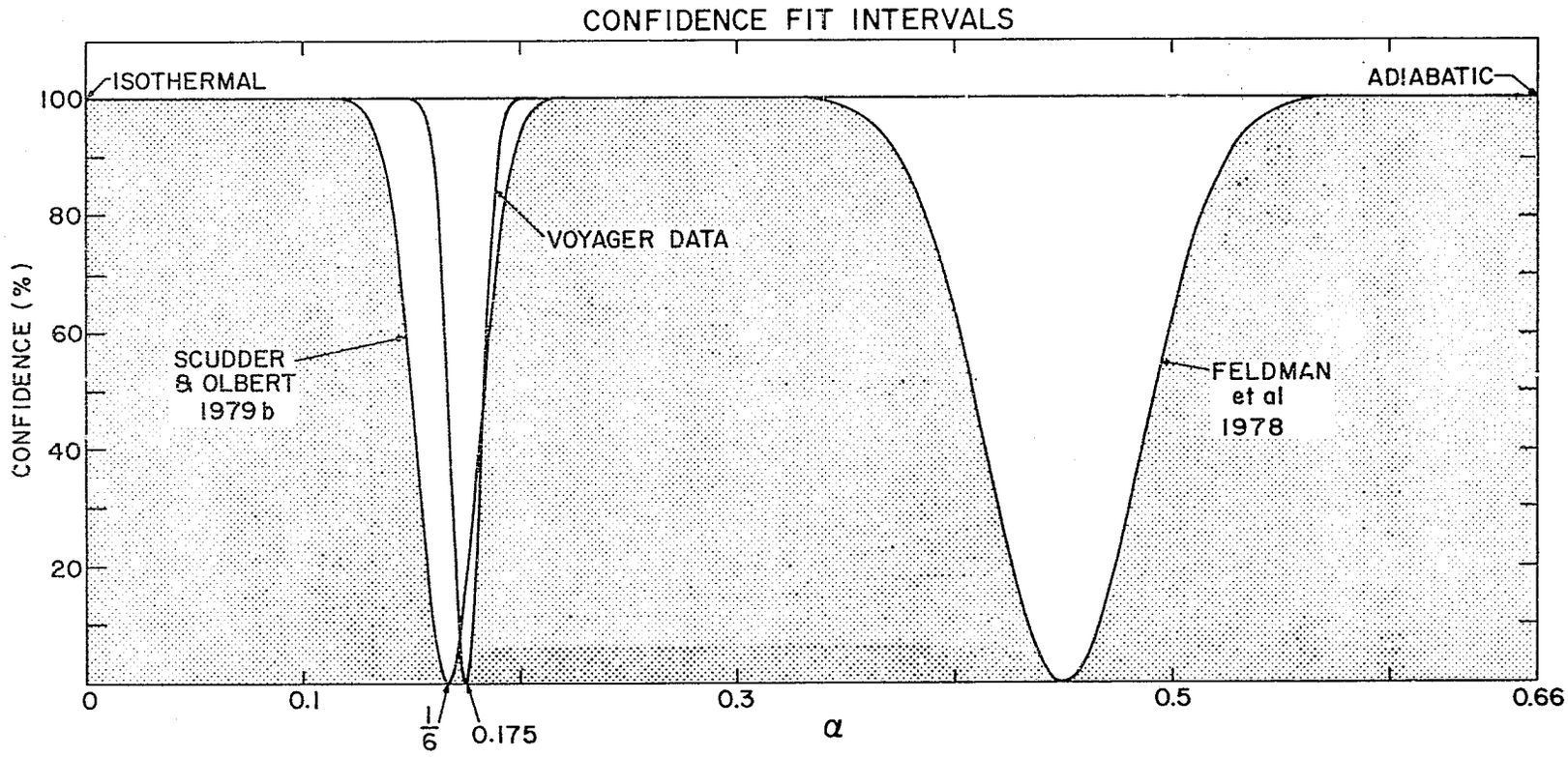
CONFIDENCE FIT INTERVALS
ISOTHERMAL
ADIABATIC
100
80
60
40
20
CONFIDENCE (%)
VOYAGER DATA
SCUDDER
& OLBERT
1979 b
FELDMAN
et al
1978
0
0.1
1/6
0.175
0.3
0.5
0.66
α

Figure 3